LAHIRI, A.K. and PAL, S. Foaminess of slag: cause and control. *VII International Conference on Molten Slags Fluxes and Salts,* The South African Institute of Mining and Metallurgy, 2004.

Foaminess of slag: cause and control

A.K. LAHIRI and S. PAL
Department of Metallurgy, Indian Institute of Science, Bangalore, India

Most of the compounds present in slag are surface active. This gives rise to foaminess of slag. The foam life and foaming index are normally determined by the draining rate of slag through the plateau border, so the foaming index is directly proportional to slag viscosity and inversely proportional to slag density and bubble diameter. When a small amount of a strong surface active compound like P_2O_5 or Cr_2O_3 is present in slag, however, the foam life increases significantly and the above relationship is not obeyed. The strong surface active compounds reduce the draining rate from the film between the adjacent bubbles so the film draining controls the life of the foam. The thickness of the film, Marangoni force, viscosity of the slag, and diffusion of surface active compounds determine the film draining rate. The interplay of these factors leads to very low or high film draining rates and affects the film and foam stability significantly.

Keywords: slag, foam, foaming index, film draining

Introduction

Slag foaming is common to all iron and steel making processes. It forms in the dripping zone of the blast furnace and creates problems in smelting of vanadium-bearing titanomagnetite ores[1]. In bath smelting processes, foamy slag separates the metal from the oxidizing atmosphere. It helps in rapid heat transfer to the metal from the post-combustion zone and maintains reducing conditions in the melt[2–4]. In BOF, a number of fine metal droplets dispersed in slag foam increases the reaction rates. Sometimes however, foamy slag leads to slopping, causing metal loss and interruption in converter operation. Foamy slag practice is followed in electric arc furnace to improve the process efficiency. It shields the refractory from the arc and metal from the furnaces atmosphere, and helps in stabilizing the arc. Foaming is found in hot metal pretreatment such as desiliconization, dephosphorization and desulphurization. Slag foam is formed during conversion of copper and nickel matte and sometimes it creates operational problems[5].

Fruehan and his associates[6–10] systematically measured and correlated the foaming characteristics for different slags of importance to iron and steelmaking. To quantify the foaming characteristics, they measured the foaming index, defined as

$$\sum = h/u \qquad [1]$$

where h is the height of the foam at steady state when gas with superficial velocity u is passed through it. The foaming index is independent of gas velocity and is related to slag properties and bubble diameter. Zhang and Fruehen[9] obtained the following empirical equation by correlating the experimental results obtained by their group

$$\sum = 115\mu^{1.2}/\left(\sigma^{0.2}\rho\, d_b^{0.9}\right) \qquad [2]$$

where μ, σ and ρ are respectively the viscosity, surface tension and density of slag and d_b is the bubble diameter. Besides the foaming index, foam stability is sometimes measured in terms of foam life, i.e., the time required to collapse foam by a definite height. Both foam life and foaming index are the same for foam of uniform void fraction[6].

Ghag *et al.*[11] measured the foaming index of a water-glycerol system in the presence of the strongly absorbent surfactant, sodium dodecylbenzene sulphonate (SDBS). They correlated the measured values[12] by the following relation:

$$\sum = 1\times10^6\left(\mu E_{eff}\right)/\left[(\rho g)^2 d_b^{\,3}\right] \qquad [3]$$

E_{eff} is the effective elasticity resulting from the adsorption of surface active species. This empirical equation shows that the foaming index is inversely proportional to d_b^3 in contrast to approximately d_b in Equation [2], besides which surface elasticity also has a major role. Hara *et al.*[13] found that bulk and surface viscosities of the Na_2O-P_2O_5 system are almost same. Thereby the concept of surface elasticity is not always applicable for a slag system.

Pilon[14] analysed the foam heights reported for slags, water-glycerol with SDBS and 75% SiO_2-15% Na_2O-10% CaO glass using a semi-empirical approach. They proposed

$$h = 2905\sigma\left[\mu(u-u_m)\right]^{0.8}/\left[(d_b/2)^{2.6}(\rho g)^{1.8}\right] \qquad [4]$$

where u_m is the minimum superficial velocity of gas for foam formation. The equation shows that the foaming index depends on gas velocity and foam height increases with surface tension. Both these observations are not in tune with Equations [2] and [3].

Recently Lahiri and Seetharaman[15] showed that for uniform bubble size, the foaming index is given by

$$\sum = C\mu/(\rho d_b) \qquad [5]$$

C is determined by the gas fraction in the foamy slag, bubble shape. and ratio of bulk to surface viscosity of slag. Equation [5] correctly represents the data reported by Fruehan and his associates[6–10] when C = 150.

The behaviour of foamy slag is sometimes very complex. Cooper and Kitchener[16] found that the foam stability increases very significantly with an increase in P_2O_5 in the $CaO\text{-}SiO_2\text{-}P_2O_5$ system till it is about 3 per cent. A further increase of P_2O_5 does not affect the foam stability. Kim[17] reported that the foaming index exhibits a maximum at about 3 per cent P_2O_5 in MgO saturated $CaO\text{-}SiO_2\text{-}30FeO\text{-}P_2O_5$ system. He further showed that the foaming index of the MgO saturated $CaO\text{-}SiO_2\text{-}30FeO\text{-}CaF_2$ system decreases with the addition of CaF_2 up to about 5 per cent. Further addition of CaF_2 increases the foaming index. Swisher and McCabe[18] observed that foam stability has a sharp peak at about 0.4 per cent Cr_2O_3 in $CaO\text{-}SiO_2\text{-}Cr_2O_3$ system with $CaO/SiO_2 = 0.64$. This corresponds to the liquid immiscibility region. Kitamura *et al.*[19] found the highest foaminess near silica saturation in $Fe_2O_3\text{-}MnO\text{-}CaO\text{-}SiO_2$ melts. But in a silica saturated region, the foaminess decreased. Obviously none of the models mentioned above can adequately explain these observations, but understanding of the cause of these behaviours will help in the control of foaming.

Foam formation

It is well known that the presence of surface active elements are essential for the formation of stable foam. When a bubble comes on the surface of a liquid, it carries a thin film of liquid along with it. The top surface of the bubble comes in contact with the liquid surface first, so the concentration of surfactant is highest at the top of the film and consequently surface tension is lowest. In the downward direction along the height of the film, the solute concentration gradually moves towards the bulk concentration, leading to an increase of surface tension. So a surface tension gradient is set up in the film around the bubble such that there is an upward force. This Marangoni force prevents fast draining of liquid from the film and makes the bubble reside on the surface for sometime. A stable foam forms on the surface of liquid if other bubbles join the first bubble before it bursts due to liquid draining from the film. Obviously the liquid draining time is insignificant in the absence of the Marangoni force since there is no resistance to the flow and thereby stable foam cannot form in the absence of surfactant. The mechanism indicates that below a minimum gas velocity or bubble formation rate, a stable foam cannot form. u_m in Equation [4] is this minimum velocity for foam formation. Obviously u_m depends on the Marangoni force. As the gas velocity increases, foam volume increases. At any gas velocity, the foam volume is determined by the following balance equation:

$$\text{Rate of foam volume change} = \text{rate of gas injection} - \text{rate of gas escape due to bubble rupture} \quad [6]$$

As a first approximation, bubble rupture rate can be assumed to be proportional to the number of bubbles. Hence

$$\text{Rate of volume change due to bubble rupture} = kNv_b \quad [7]$$

where v_b is the average volume of a bubble, N is the total number of bubbles and k is the rate constant for bubble rupture. Total volume of foam and bubble is related by

$$\varepsilon = Nv_b / v \quad [8]$$

where ε is the average void fraction and v is the volume of foam.

Using Equations [7] and [8], Equation [6] can be written as

$$dv/dt = Q - k\varepsilon v \quad [9]$$

where Q is the rate of gas injection. If foam is produced in a container of uniform cross section area, the above equation becomes

$$dh/dt = u_s - k\varepsilon h \quad [10]$$

So at steady state, the foaming index defined by Equation [1] becomes

$$\sum = 1/(k\varepsilon) \quad [11]$$

Equation [11] shows that the foaming index is independent of superficial gas velocity when both k and ε are independent of superficial gas velocity.

Bubble rupture

The foam consists of polyhedral bubbles separated by thin liquid films or lamellae. Three adjacent films meet at a plateau border channel, which is a duct of approximately triangular cross-section. The curvature of the plateau border walls produces a suction, which drives the liquid from the film to the plateau border. As the liquid is drained out of the film, it becomes thinner till it reaches equilibrium or critical thickness, which is between 5 and 100 nm. At this film thickness, the repulsion between adsorbed surface layers compensates the capillary pressure and van der Waals attraction force. This thin film ruptures due to thermal or mechanical fluctuation. So the bubble collapse time is the sum of drainage time and the lifetime of critically thin film[20].

Usually the drainage rate of liquid through the plateau border channels controls the film draining rate. The liquid moves through the plateau border due to gravity. The drainage rate through the plateau border per unit cross sectional area of foam is[21]

$$q = (3/30) n\, a_p\, n_p\, u\, d_b \quad [12]$$

where n, a_p, n_p, u, and d_b are respectively the number of bubbles per unit volume of foam, cross-sectional area of a plateau border channel, number of plateau borders per bubble, drainage velocity, and average diameter of bubble. The drainage velocity is given by[22]

$$u = c_v a_p / \left[\left(20\sqrt{3}\right)\mu\right]\left[\rho g - \left(\partial p/\partial z\right)\right] \quad [13]$$

where z is the distance in the vertical downward direction, ρ, μ, and p are respectively density, viscosity, and pressure in liquid, and g is the acceleration due to gravity. c_v is a polynomial of inverse of dimensionless surface viscosity $(\mu\sqrt{a_p})/\mu_s$ where μ_s is the surface viscosity $\partial p/\partial z$ is the pressure gradient in the plateau border, which is normally insignificant.

If the lifetime of critically thin film is very small, the bubbles will collapse when the liquid entrapped between two successive layers of bubbles is drained out. So Equations [12] and [13] determine the rate of bubble collapse when the film draining is not rate controlling. Equation [5] determines the foaming index for this case.

Film draining

Normally the film draining rate is not important for the bubble rupture. But when the film thickness becomes small and the surfactant distribution on the film results in a surface force opposing the fluid flow, the film draining rate

can be rate controlling. To illustrate this, we consider a simple case of a vertical film falling under the action of gravity. Figure 1 schematically shows the system. The velocity distribution of liquid in the film is given by:

$$\rho(\partial v/\partial t) = \mu\left(\partial^2 v/\partial y^2\right) + \rho g \quad [14]$$

with the initial and boundary conditions:

$$\text{at } t = 0,\ \text{for} -\delta \le y \le \delta,\ v = 0 \quad [15a]$$

$$\text{at } t > 0,\ y = \pm\delta, -\mu(\partial v/\partial y) = d\sigma/dx \quad [15b]$$

In dimensionless form, Equations [14] and [15] become

$$\partial\varphi/\partial\tau = \partial^2\varphi/\partial\xi^2 + 1 \quad [16]$$

with boundary conditions,

$$\text{at } \tau = 0 \text{ and } -1 \le \xi \le 1,\ \varphi = 0$$

$$\text{at } \tau > 0, \text{ and } \xi = \pm 1,\ \partial\varphi/\partial\xi = \beta$$

where $\xi = y/\delta$, $\tau = (\mu t)/(\rho\delta^2)$, $\varphi = (\mu v)/(\rho\delta^2)$ and $\beta = [1/(\rho g\delta)](d\sigma/dx)$ are respectively dimensionless distance, time, velocity and Marangoni force. Figure 2 shows that the average dimensionless draining velocity across the cross section of the film increases with time and it is strongly dependent on values of β. When δ = 1, the upward force due to surface tension gradient counter balances gravity force, and draining velocity becomes zero. As the liquid drains out from the film two phenomena take place. Firstly the film thickness decreases due to film draining and secondly $d\sigma/dx$ decreases due to diffusion of surfactants. The former increases β and the later decreases it. The definition of dimensionless velocity φ indicates that a slight reduction of film thickness will reduce the draining velocity very significantly. The above results reveal that if a large concentration gradient of surfactant is present on the film, the film draining rate is determined by film thickness, Marangoni force, viscosity and diffusion of surfactant. Because of the interplay of these factors, the draining velocity could be very low and control the bubble rupture.

If the concentration of surfactant on the film is very high, the surfactant can form a thin visco-elastic film or membrane at the gas-liquid interface. So the velocity of the liquid at the gas-liquid interface becomes zero under no slip condition. This type of situation is often encountered in an aqueous system containing a small amount of strong surfactant and these foams can exist as dry foam even after liquid is drained out of the film. Figure 2 shows that the draining velocity becomes very small when a film is formed at the gas-liquid interface. In this case, film draining velocity attains steady state in a very short time.

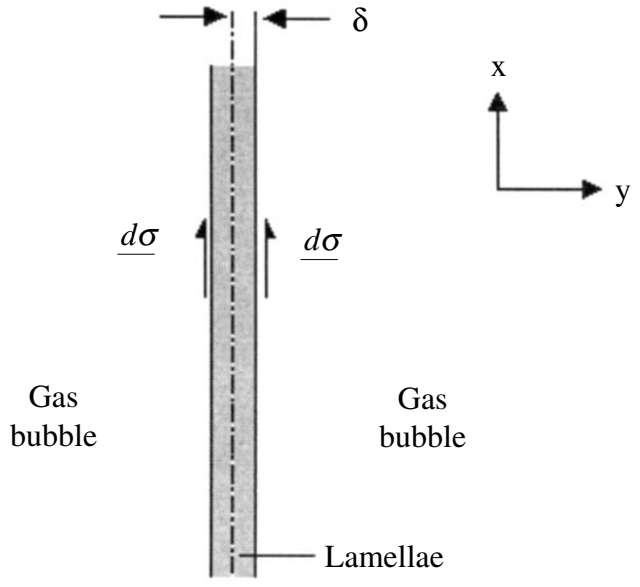

Figure 1. Schematic diagram of a vertical film falling under gravity and surface forces acting upward

Application for slag

Figure 3 shows[23] the effect of different solutes on the surface tension of $CaO\text{-}SiO_2$ systems. All solutes shown in Figure 3 are surface active except Al_2O_3. The data of the $CaO\text{-}Al_2O_3\text{-}SiO_2$ system show that SiO_2 is surface active for the $CaO\text{-}Al_2O_3$ system. Thereby it can be concluded that slags have inherent foaminess. P_2O_5, Cr_2O_3, CaS, V_2O_5 and CaF_2 are highly surface active compared to SiO_2 or Fe_xO. So a concentration gradient of these compounds in the film can significantly lower the film draining rate and increase the foam height.

The data of Cooper and Kitchener[16] for the $CaO\text{-}SiO_2\text{-}P_2O_5$ system show that dσ/dC is about-11mNm^{-1}%mol^{-1} due to the addition of P_2O_5 in slag of CaO/SiO_2 = 0.77. Calculation shows that for a film thickness of 1 μm, β ≈ 1

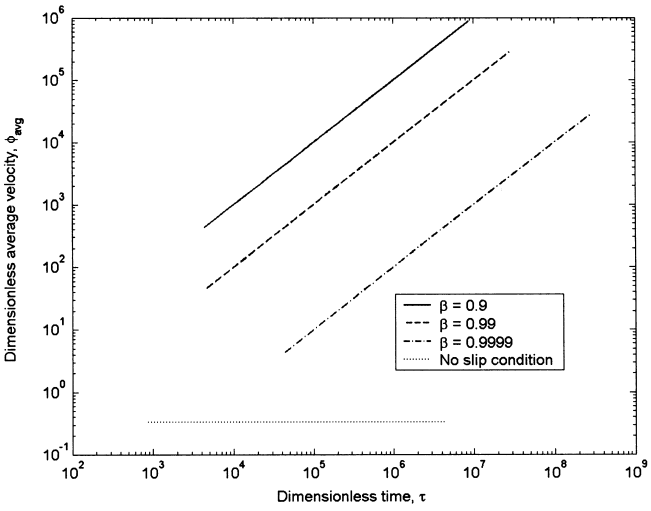

Figure 2. Dimensionless average draining velocity through the film in the presence of surface tension gradient

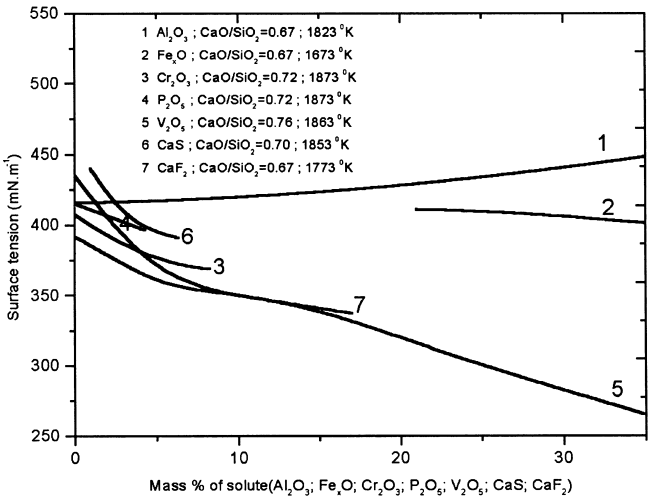

Figure 3. The effect of different solutes on the surface tension of $CaO\text{-}SiO_2$ system[23]

when dc/dx = 20 ppm/mm. So under this condition, foam life could be determined by film draining and it will be much higher than that given by Equation [5]. Furthermore, once the surface gets saturated with P_2O_5, the film draining rate could be very small as shown in the lower-most line of Figure 2 and further addition of P_2O_5 will not affect the foam life. The observation of Cooper and Kitchener[16] shown in Figure 4 supports this mechanism. Obviously in different slags, both dσ/dC and dc/dx are different and will vary with slag composition, leading to variation in foam behaviour. Figure 4 shows that the effect of P_2O_5 in different slags is not the same, although its addition increases the foam life or foaming index considerably.

Figure 5 shows the foam life reported by Swisher and McCabe[18] for the $CaO-SiO_2-Cr_2O_3$ system dσ/dC is about-20 $mNm^{-1}\%mol^{-1}$ when a small amount of Cr_2O_3 is added in $CaO-SiO_2$ system[18]. Since this is almost twice that of P_2O_5 in the $CaO-SiO_2$ system, the effect of Cr_2O_3 addition on foaming index is very high. At about 0.4 per cent Cr_2O_3, the $CaO-SiO_2-Cr_2O_3$ system separates into two liquids and therefore dσ/dC = 0. This results in an increase of film draining rate and a rapid decrease in foam life. Kitamura *et al.*[19] found the highest foaminess near silica saturation in Fe_2O_3-MnO-CaO-SiO_2 melts as shown in Figure 6. But in the silica saturation region, the foaminess decreased. This also could be attributed to the absence of the Marangoni force. The gradual increase in foam life beyond about 1per cent Cr_2O_3 as shown in Figure 5 could be due to increased viscosity of slag in the two phase region.

CaF_2 affects the slag property in two different ways. It reduces both the viscosity and surface tension of slag. The former reduces the foaming index, whereas later increases it. So the net effect is quite complex as shown in Figure 7.

Conclusion

When a strong surface active agent is present in slag, the film draining rate is very low because of the Marangoni force and foam life is determined by the film draining rate. The foaming index of these foams cannot be calculated by the available relationships.

The foaming index of two-phase slags, which are saturated with the surface active reagent, is very low because of absence of the Marangoni force.

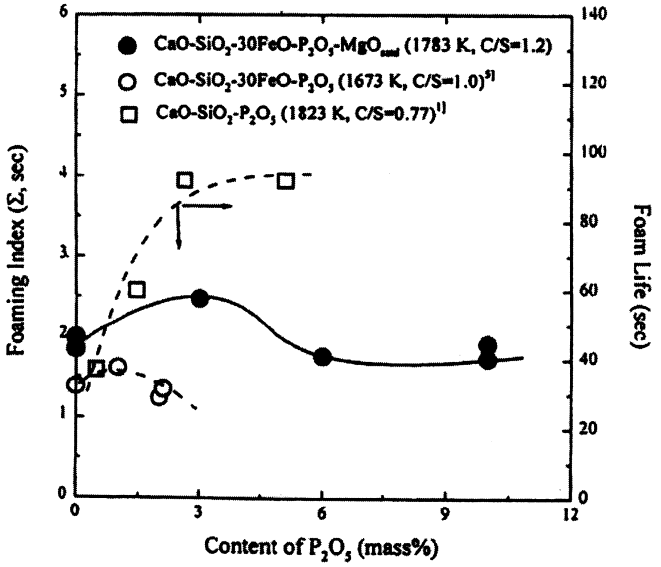

Figure 4. Effect of P_2O_5 on foaming index of different slags. Kim[17]

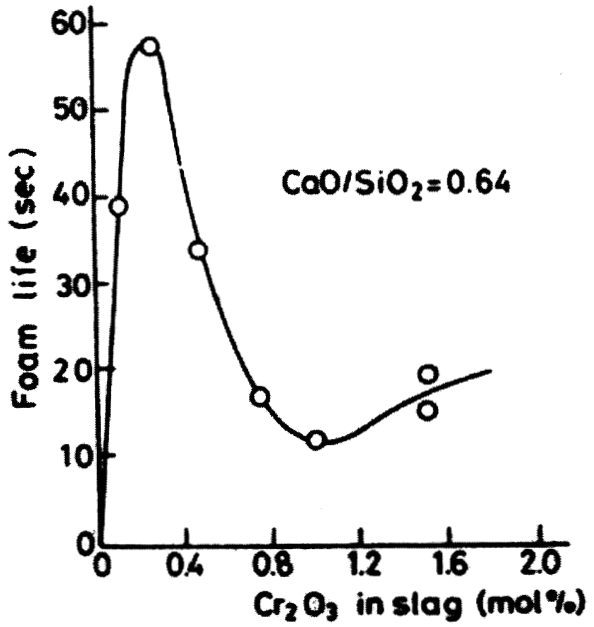

Figure 5. Effect of Cr_2O_3 on foaming index of $CaO-SiO_2-Cr_2O_3$ systems[18]

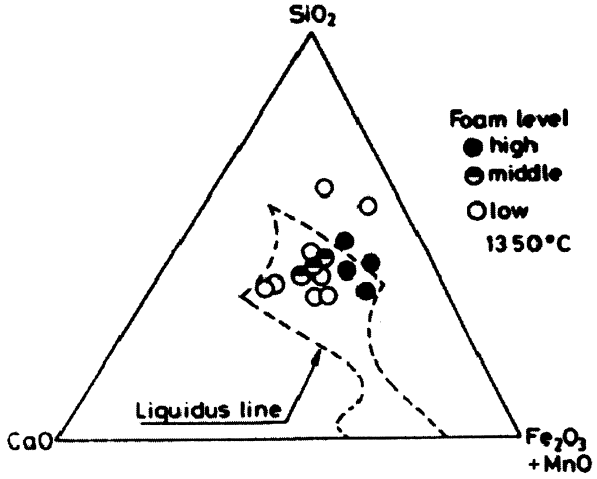

Figure 6. Foaming height in $CaO-SiO_2-Fe_2O_3$-MnO system[19]

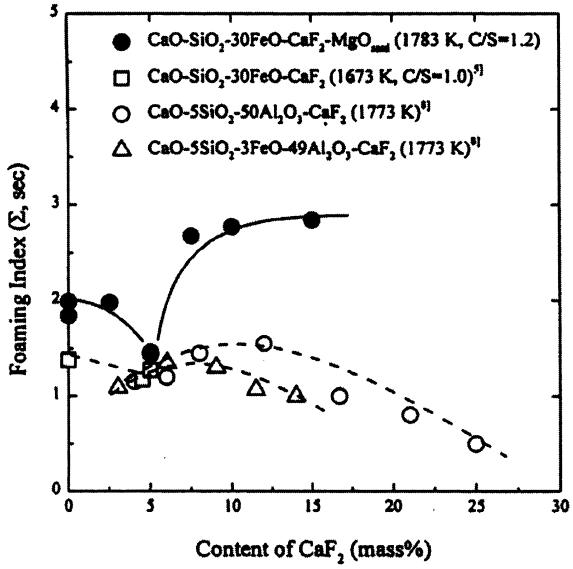

Figure 7. Foaming index of slags containing CaF_2. Kim[17]

References

1. DIAO, R. *Iron and Steel* (Peking), vol. 34, no. 6. 1999. pp. 12–14.
2. KATAYAMA, H., OHNO, T., YAMAUCHI, M., MATSUO, M., KAWAMURA, T., and IBARAKI, T. *ISIJ Int.*, vol. 32, 1992. pp. 95–101.
3. LAHIRI, A.K. *Proc. Workshop Prod. Liq. Iron using coal,* Ray, H.S., Dey, D.N., Paramguru, R.K., and Jouhari, A. K. (eds.) Regional Research Lab, Bhubaneswar, India, 1994. pp. 149–153.
4. DONATO, A.D., MALGARINI, G., OETERS, F., and ZHANG, L. *Steel Research*, vol. 70, 1999. pp. 386-394.
5. ROSET, G.K., MATOUSEK, J.W., and MARCANTONIO, P.J. *JOM*, vol. 44,1992. pp. 39–42.
6. ITO, K. and FRUEHAN, R.J. *Metall. and Mater. Trans. B,* vol. 20B, 1989. pp. 509–514.
7. JIANG, R. and FRUEHAN, R.J. *ibid*, vol. 22B, 1991. pp. 481–489.
8. ROTH, R.E., JIANG, R., and FRUEHAN, R.J. *Trans. ISS*, vol. 19, Nov. 1992. pp. 55–63.
9. ZHANG, Y. and FRUEHAN, R.J. *Metall. and Mater. Trans B*, vol. 26B, 1995. pp. 803–812.
10. JUNG, S. and FRUEHAN, R.J. *ISIJ Int.*, vol. 40, 2000. pp. 348–355.
11. GHAG, S.S., HAYES, P.C., and LEE, H.G. *ISIJ Int*., vol. 38, 1998. pp. 1201–1207.
12. GHAG, S.S., HAYES, P.C., and LEE, H.G. *ISIJ Int*., vol. 38, 1998. pp. 1208–1216.
13. HARA, S., KITAMURA, M., and OGINO, M. *ISIJ Int.*, vol. 30, 1990. pp. 714–721.
14. PILON, L., FEDOROV, A. G., and VISKANTA, R. J *Colloid Interface Sci*., vol. 242, 2001. pp. 425–436.
15. LAHIRI, A.K. and SEETHARAMAN, S. *Metall. and Mater. Trans B*. vol. 33B, 2002. pp. 499–502.
16. COOPER, C.F. and KITCHENER, J.A. JISI, vol. 193, 1959. pp. 48–55.
17. KIM, H., MIN, D., and PARK, J. *ISIJ Int*., vol. 41, 2001. pp. 317–323.
18. SWISHER, J.H. and MCCABE, C.L. *Trans TMS-AIME*, vol. 230, 1964. pp. 1669–1675.
19. KITAMURA, S., OGAHIRA, K., TANAKA, S., and DOI, M. *Tetsu-to-Hagane*, vol. 69, 1983. pp. S31.
20. HRMA, P. *J Colloid Interface Sci*. vol. 134, 1990. pp. 161–168.
21. NARSIMHAN, G. and RUCKENSTEIN, E. *Langmuir*, vol. 2, 1986. pp. 494.
22. DASAI, D. and KUMAR, R. *Chem. Eng. Sci.* vol. 37, 1982. pp. 1361.
23. LAHIRI, A.K., YOGAMBHA, R., DAYAL, P., and SEETHARAMAN, S. *Proc. Mills symposium: Metals, Slags, Glasses*: *High Temperature Properties and Phenomena*; Aune, R.E., and Sridhar, S. (eds); Institute of Metals, London, 22–23 August 2002. vol. 1, pp. 231–238.